# Ink temperatures in resistive ribbon thermal transfer printing

by T. C. Chieu O. Sahni

A knowledge of ink temperatures is important in thermal transfer printing technologies. This paper reports on an experimental technique which uses an infrared radiometric microscope to measure the temperature of ink deposited by the resistive ribbon process on transparent substrates. A detailed examination has been made of the spatial and temporal profiles of ink temperatures as a function of input current. printing speed, substrate materials, and number of active electrodes. The results on a ®Kapton substrate permit estimation of the ink temperatures reached during printing on paper. The peak ink temperatures are observed to depend linearly on input current and inversely on an approximately linear function of writing speed from 2 to 8 inches per second. Based on a phenomenological model, these results lead to a functional relationship among speed, print current, and ink temperature during printing. The model permits projections to be made of the current required over a wide range of printing speeds.

### 1. Introduction

Thermal transfer (T2) printing has emerged as one of the leading nonimpact printing techniques for low-end

**°Copyright** 1985 by International Business Machines Corporation. Copying in printed form for private use is permitted without payment of royalty provided that (1) each reproduction is done without alteration and (2) the *Journal* reference and IBM copyright notice are included on the first page. The title and abstract, but no other portions, of this paper may be copied or distributed royalty free without further permission by computer-based and other information-service systems. Permission to *republish* any other portion of this paper must be obtained from the Editor.

applications because of its simplicity, high reliability, and quietness. The serial T2 printer [1] is limited in speed by the time constant of the thermal head. This has led to the development of the T2 line printer for higher speeds of the order of a few pages per minute [1]. The development of resistive ribbon thermal transfer printing [2–6] has greatly improved the inherent speed cabability of a serial head, which is limited in the T2 printer by the large thermal time constant of the massive head. Moreover, it allows quality printing on a wide variety of papers at speeds which are competitive with those of wire matrix impact printing.

The resistive ribbon printing process involves generating a thermal transient within the resistive ribbon itself which effectively softens the ink, thereby reducing the shear strength of the localized heated area of the ink and causing it to transfer to the paper. The strength of the bond between hot ink and paper fibers depends on the head pressure and the peak temperature of the softened ink during the thermal pulse. Further, the area of the printed element also depends on the ink temperature. Thus the control and knowledge of ink temperatures are important in understanding and improving the reliability and performance of this technology.

This paper presents a detailed report of dynamic measurements of ink temperatures in thermal transfer printing technology. The experimental technique involves using an infrared (IR) radiometric microscope to measure the temperature of ink deposited by the resistive ribbon process on a transparent substrate. Detailed measurements were made of the spatial and temporal temperature profiles of ink during printing. Further, the peak ink temperatures were measured as a function of the input current, printing speed, substrate materials, and number of active electrodes. The dependence on input current and printing speed is

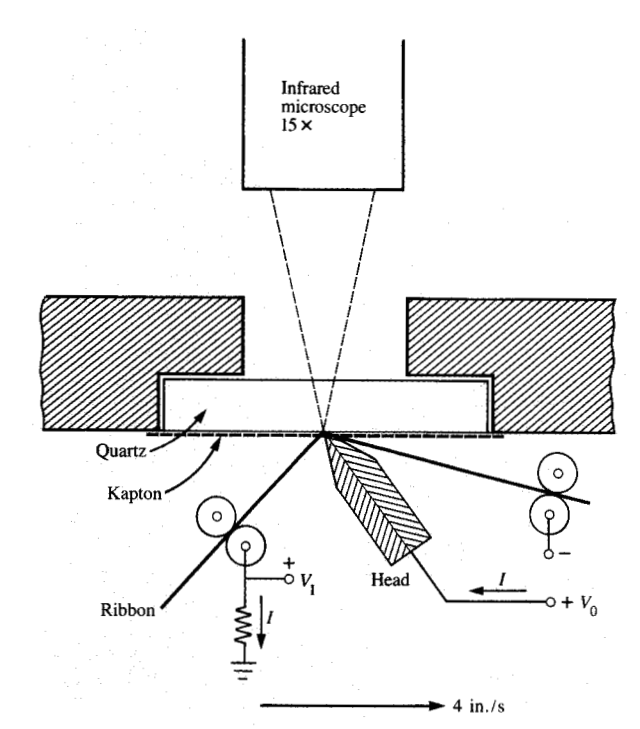


Figure 1
Schematic of experimental apparatus.

explained on the basis of a phenomenological model of three-dimensional heat conduction with moving heat sources. This model permits projections to be made of the current required for achieving equivalent ink temperatures over a wide range of printing speeds.

# 2. Experimental techniques

The ink temperature measurements were made with a Barnes infrared radiometric microscope and an experimental robot capable of varying print current and printing speed over a fairly wide range. The experimental apparatus is shown schematically in Figure 1. The microscope consists of an objective (with 15× magnification) for collecting target energy, a visible light channel equipped with an eyepiece for viewing the target, and an infrared optical channel which includes a liquid nitrogen dewar and an indium antimonide detector. The robot consists of a printhead mounted on a moving ribbon cartridge, and a flat platen with a slot cut out for an IR transmitting window. The robot permits printing on the transparent window while the IR microscope is focused on the window-ink interface. Infrared emission from the hot ink is measured by the microscope with a spatial resolution of 35  $\mu$ m. The printhead has a flat edge on which there is an array of tungsten electrodes approximately 2 mils  $(50 \mu m)$  wide arranged with a center-to-center spacing of

approximately 4 mils ( $100 \mu m$ ). The electrode tips are in pressure contact ( $\sim 150 \text{ kg/cm}^2$ ) with the ribbon as the printhead is pushed against the platen. The contact area is estimated to be nominally  $46 \times 50 \mu m^2$  for a new head; it is expected to vary with age and the condition of the head. The resistive ribbon consists of a carbon-loaded (conducting) polycarbonate layer approximately  $15 \mu m$  thick, a thin aluminum layer ( $\sim 100 \text{ nm}$ ) acting as the ground return plane for the current, and an ink transfer layer which is 4 to 6  $\mu m$  thick.

The IR transmitting substrate in this experiment is a 1.7-mm-thick quartz window. The substrate can be altered by placing a 75- $\mu$ m-thick \*Kapton [7] sheet on top of the quartz window. The measurements of ink temperatures on Kapton, which has a thermal conductivity and heat capacity comparable to those of paper, permit an estimation to be made of the ink temperatures reached during actual printing (at least on very smooth papers with a reasonably good thermal contact with the ink).

The measurement strategy was to focus the IR microscope on the observation window, on which the moving head printed a short stripe pattern usually consisting of five activated electrodes. To avoid heating the head, this pattern was typically one character length of 2.5 mm, and the observation point was normally close to the trailing end of the stripe pattern. The ink temperatures were measured by recording the thermal pulse as a function of time, as the printhead moved past the observation point. The voltage output from the IR microscope, which is proportional to the emitted radiance of the ink, was recorded using a Model 4094 Nicolet digital oscilloscope. The print current pulse and the total voltage across the ribbon were recorded simultaneously to keep track of the power delivered to the resistive ribbon. The ac operation mode of the IR microscope was used to give a fast response of the transient temperatures of the ink deposited on the substrate. The temperature calibrations of the IR microscope were done by focusing the microscope on the tip of an ink-coated chromelalumel thermocouple, spark-welded on a heat gun acting as the thermal source.

In spite of the good response time ( $\sim 8~\mu s$ ) and high temperature resolution ( $<1^{\circ}$ C) of the IR microscope, the measured ink temperatures could not be determined to better than 10°C. This was due to the inability of the moving printhead, from run to run, to retrace precisely its motion past the fixed observation point. Any slight mechanical jitter in the moving head changes the relative position of the fixed observation point with respect to the center of the printing electrode, and this gives the small random variation in the repeatability of the temperature measurements. To overcome this problem, a statistical average of the measured ink temperatures has been carried out such that each data point reported in this article represents the average of a number of data points (10 to 15) which usually formed a

preferential cluster within a total set of 15 to 20 observations.

The spatial variation of peak ink temperatures in a direction orthogonal to the print direction was obtained by moving the observation point of the IR microscope laterally across the stripe ink pattern. The ink directly under the electrodes gets very hot during printing and melts to a lowviscosity fluid which is then squeezed out laterally due to the pressure under the head. This leaves a thinner layer of ink deposited on the substrate immediately under the electrodes. These optically distinct tracks formed by the ink below the moving electrodes were used to identify the position of the electrodes in the measurements. A closer examination of these ink tracks shows a random distribution of extremely hot spots of a few micrometers in size under the electrodes. The ink at these spots is significantly thinner than in the adjoining areas of the tracks. The temperatures at these distributed hot spots were not determined because of the finite spatial resolution of the IR microscope, which encompasses a much larger area in its field of view to give only an effective value of ink temperature under the electrodes.

### 3. Results and discussion

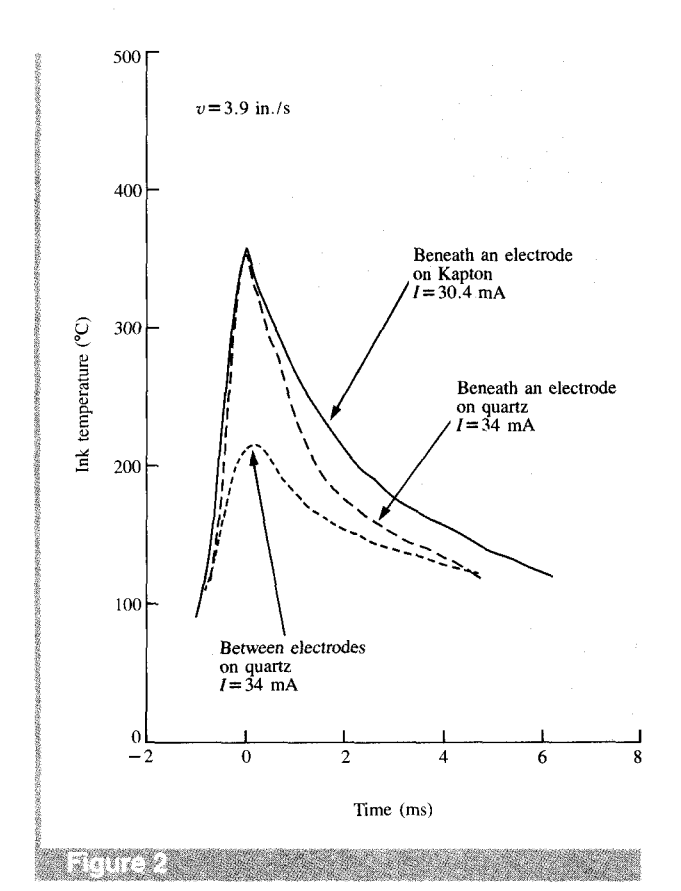
In subsequent sections, we present the temporal and spatial profiles of ink temperatures on quartz and Kapton substrates, and show results of peak ink temperatures as a function of print current for various printing speeds and numbers of active electrodes. Finally, we describe a phenomenological model of three-dimensional heat conduction with finite heat sources moving in a composite medium. The calculated temperatures are fitted to the experimental data, and then analytical projections are made of the current required for obtaining equivalent ink temperatures over a wide range of printing speeds.

• Temporal and spatial temperature profiles

The temporal profiles were obtained by recording the time decay of the temperature of the ink deposited on the substrate as the printhead moves past the observation point.

Figure 2 shows two different temporal profile curves corresponding to the temperature of the ink immediately under an active electrode and between active electrodes on Kapton substrate for a print current of 30.4 mA and a printing speed of 3.9 in./s (10 cm/s). It is observed that the ink located between two fired electrodes also peaks to a fairly high temperature (~230°C), although this temperature is much lower than that under an active electrode (~380°C). The relatively high values of the temperatures at the ink layer are comparable to the values predicted by the lumped-element model [8, 9].

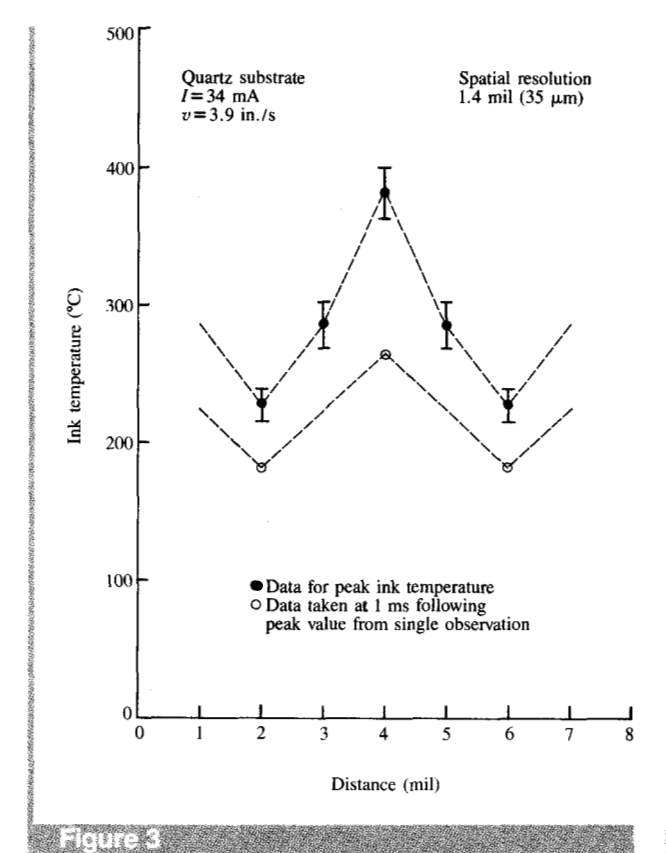
The variation of these peak ink temperatures as a function of distance in the lateral direction is illustrated in Figure 3 for a quartz substrate. Also included in this figure is the



Temporal profiles of ink temperature underneath an electrode and between electrodes for quartz and Kapton substrates.

spatial variation of ink temperatures at about 1 ms following the peak, which represents an estimate of the time required for the ribbon to peel away from the paper during printing. Of significance is the fact that the ink temperatures between electrodes at this time are still much higher than the inksoftening temperature, and that the spatial variations become much smaller due to thermal diffusion. Undoubtedly, these ink temperatures equilibrate rapidly downstream, with an almost uniform ribbon temperature throughout the thickness, as corroborated by the similar range of temperatures measured at the top surface of a ribbon emerging from under the electrode [10].

• Input current and printing speed dependences
In printing experiments with constant current drivers, the two important independent variables are the input current and printing speed. The electrical current is the origin of the power dissipated in the ribbon and thus is the source of the heating of the ink layer. Measurements of the ink temperatures as a function of input current thus provide us information concerning the distribution of electrical power in the ribbon. On the other hand, information concerning



Spatial profiles of ink temperature on quartz substrate.

the dependence of ink temperatures on the printing speed is important in understanding the thermal system sufficiently well to predict the electrical power requirements for the future extension of the resistive ribbon technology to higher printing speeds. We have therefore measured the ink temperatures as a function of input current for various printing speeds. The results are presented in **Figure 4** for a Kapton substrate; for comparison, the data on a quartz substrate are also included in the inset of this figure.

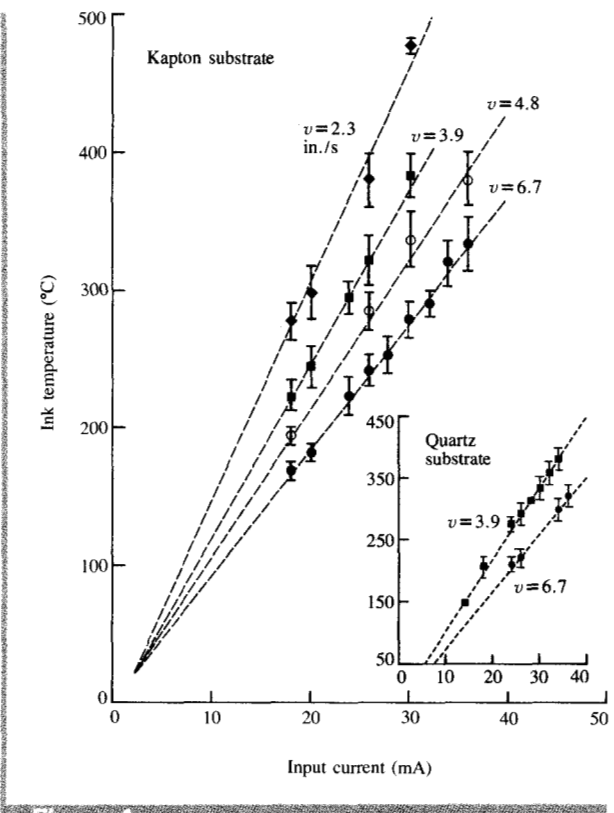
The experimental plots show a linear dependence of peak ink temperatures on input current. The linear dependence can be understood in terms of temperature rise caused by heating power, which is proportional to the input current. This input power for heating the ink is thought  $\{11, 12\}$  to be generated mainly at the polycarbonate-aluminum interface, where the tunneling across the thin interfacial barrier layer gives rise to the nonlinear current-voltage (I-V) characteristics of the ribbon. There is also a secondary contribution of heat input from the nonlinear interface resistance formed by the sliding electrode-ribbon contact at the top surface.

The curves of Fig. 4 have a decreasing slope for increasing speed of the printhead, and all of them intersect at a

constant current value of approximately 2 mA at ambient temperature. The convergence of these plots at a constant current value at ambient temperature can be explained by postulating a small loss in current due to lateral spreading in the ribbon, a loss term which is nearly independent of printing speed.

A comparison of these data for Kapton and quartz substrates shows that the peak ink temperatures reached on Kapton are higher than those on quartz for the same input current and printing speed. This observation is expected, since the Kapton material has a lower thermal conductivity which restrains the heat flux from flowing across the interface, thus resulting in higher ink temperature. On the basis of this fact, the ink temperatures reached on rough paper during printing are expected to be even higher than those measured on Kapton.

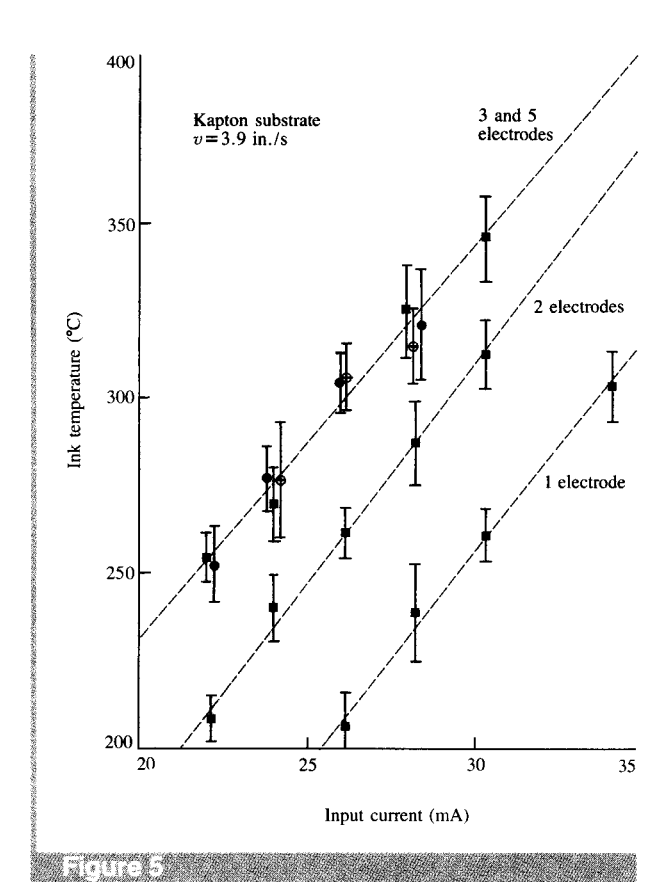
While the linear dependence of peak ink temperatures on current is clear, the functional relationship of these temperatures to printing speeds is less obvious. An empirical fit of the data shows that the inverse of these temperatures is a nearly linear function of speed within the relatively narrow experimental range. To account correctly for the dependence of the peak ink temperatures on the printing speed, a



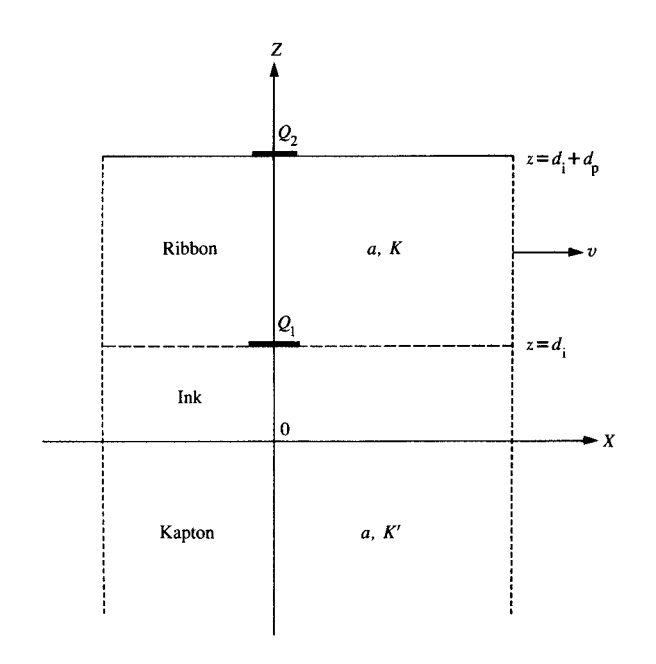
Peak ink temperatures versus input current for different printing speeds on quartz and Kapton substrates.

phenomenological model based on a moving heat source is necessary. This model is presented in a later section of this paper.

• Ink temperatures for single and multiple electrodes Because of lateral thermal interactions in the ribbon, one expects some differences to be observed in ink temperatures between the case of a single active electrode and the case of this electrode with multiple neighbors turned on simultaneously. Figure 5 shows three different sets of data for the cases of a single electrode, double electrodes, and triple electrodes. For the case of triple electrodes, the ink temperatures were taken under the center active electrode. The increase in peak ink temperatures in going from three to five electrodes is too small to be resolved by our measurement system. It is seen that significantly higher ink temperatures are found for the case of triple electrodes as compared to the other two cases, so that in order to obtain the same peak ink temperatures as with multiple electrodes, one would have to increase the input current for the case of single or double electrodes. The intersection of a family of



Peak ink temperature versus current for different numbers of active electrodes on a Kapton substrate. For the 3- and 5-electrode cases, ink temperatures were measured under the central electrode.



### Grammara.

Schematic of ribbon, ink, and substrate structure

horizontal lines with the three curves of Fig. 5 would give the required current, for a peak ink temperature of the chosen horizontal line, corresponding to the number of active electrodes.

# • Phenomenological model

A one-dimensional thermal model of a stationary heat source simulating the resistive ribbon printing process has been given by Pennington and Mitchell [4]. This early thermal model has shown the potential superiority of the resistive ribbon printing process over the conventional thermal transfer process. In order to obtain an analytical relationship among input power, printing speed, and ink temperature for the resistive ribbon printing, we have analyzed a three-dimensional heat conduction problem of a set of finite sources moving inside a composite medium. In our particular problem, the composite medium consists of a slab of ribbon layer (polycarbonate layer) with thermal diffusivity  $a_p$ , conductivity  $K_p$ , heat capacity  $C_p$ , and thickness  $d_{\rm p}$ , a slab of ink layer with thermal constants  $a_{\rm i}$ ,  $K_{\rm i}$ ,  $C_i$  and thickness  $d_i$ ; and finally the substrate material (Kapton), which can be regarded as a semi-infinite medium with thermal constants  $a_k$ ,  $K_k$ , and  $C_k$ . The heat sources  $Q_1$ and  $Q_2$  are located at the ribbon-ink interface and at the ribbon top surface, corresponding to the contributions from the polycarbonate-aluminum interface and from the contact resistance, respectively. A schematic of the ribbon, ink, and substrate structure is shown in Figure 6.

The present problem is a four-dimensional space-time problem with prescribed boundary conditions at each interface. To solve this problem, we simplify it by making the following assumptions: We assume that the ribbon layer and the ink layer are of the same medium, with thermal constants a, K, and C (= K/a), and that the substrate material has the same thermal diffusivity a as the ribbon and ink layer, but different thermal conductivity and heat capacity K' and C' (= K'/a). With these simplifying assumptions, we can now proceed to solve the heat conduction problem.

If the ribbon and ink layer is a semi-infinite medium in the  $z \ge 0$  region, the temperatures at both the  $z \ge 0$  and the z < 0 regions due to an instantaneous source Q (Joules), located at  $(x_0, y_0, z_0)$  in region  $z \ge 0$ , are given by Eqs. (1) and (2). In other words,  $T_1$ , the temperature in region  $z \ge 0$ , is that due to the original source Q together with a source of strength Q' = (K - K')Q/(K + K') located at the "image" position  $(x_0, y_0, -z_0)$ , and  $T_2$ , the temperature in region z < 0, is that for a source of strength 2KQ/(K + K') at position  $(x_0, y_0, z_0)$  [13].

Since the ribbon and ink layer is a finite slab of medium with a top insulating surface at  $z=d_i+d_p$ , we have to superimpose the above solutions by the method of images for a thermal insulating surface. In addition, we have two heat sources  $Q_1$  and  $Q_2$  located at  $(x_0, y_0, d_i)$  and  $(x_0, y_0, d_i+d_p)$ , corresponding to heat contributions from the polycarbonate-aluminum interface and the sliding electroderibbon contact, respectively, so that  $T_r(x, y, z, x_0, y_0)$ , the ribbon temperature at x, y, z in region  $0 \le z < d_i + d_p$ , is given by Eq. (3).

Equations (3–5) represent the temperatures for a composite medium due to nonmoving instantaneous sources  $Q_1$  and  $Q_2$ . The term  $T_{r1}(x, y, z, x_0, y_0)$  is attributed to the source  $Q_1$  between two boundary planes at z=0 and  $z=d_1+d_p$ , and the term  $T_{r2}(x, y, z, x_0, y_0)$  is attributed to source  $Q_2$  due to the same boundary planes. For moving heat sources with velocity v parallel to the X-axis direction, we introduce the time-space transform of  $t \to t - t'$ ,  $x_0 \to x_0 + v(t-t')$  and  $Q_1 \to q_1 dt'$ , then perform the integration of time t' from 0 to t. Finally we obtain the ribbon temperature for moving sources  $T_m(x, y, z, x_0, y_0)$  in steady state  $(t \to \infty)$  as shown in Eq. (6).

In Eqs. (7-9), the R's represent the distance from the image source to point x, y, z and  $q_1$ ,  $q_2$  are the heat inputs in watts

Equations (6–9) represent the temperatures of the ribbon and ink layer for a point electrode. To introduce the finite electrode size effect, we perform the space transform by replacing  $x_0 \rightarrow x_0 - x'$ ,  $y_0 \rightarrow y_0 - y'$ ; we integrate x' and y' over the dimension of the heat sources  $2l \times 2w$  and A for  $q'_1$  and  $q'_2$  respectively [see Eq. (10)].

Now the sources in the expression for  $T_{\rm M}(x, y, z, x_0, y_0)$  are  $q_1'$  and  $q_2'$ , which are the heat inputs in W/cm<sup>2</sup>. These

heat inputs are assumed to be directly proportional to the input current density. The proportionality constant for  $q'_1$ which is the heat input from the polycarbonate-aluminum interface, was derived from the interfacial tunneling voltage determined from static I-V measurements [11] of ribbon samples. The proportionality constant for  $q'_2$ , which is the heat input from the top surface due to the resistance of the electrode-ribbon sliding contact, was estimated in the present experiment by measuring dynamically the total voltage across the ribbon and subtracting from it the voltage drop across the ribbon thickness and the aluminum-ribbon interface (for simplicity, half of the heat generated at the top surface was assumed to be conducted instantaneously away by the moving electrode). Further,  $q'_2$  is assumed to have a print-speed dependence of  $v^{0.8}$  as obtained from a fit of the experimental data for the total voltage across the ribbon as a function of print speed at constant current values [14].

Equation (10) gives the temperature of the ribbon and ink layer for a single electrode. For an array of N electrodes in the y direction with the first electrode centered at  $x_0 = 0$  and with center-to-center spacing of  $y_s$ , the ink temperature  $T_i(x, y, z)$  at the ink-substrate interface (z = 0) is given by

$$T_{i}(x, y, 0) = \sum_{m=0}^{N-1} T_{M}(x, y, 0, 0, my_{s}).$$
 (11)

In this thermal model, a is the effective thermal diffusivity of the multilayer sandwich consisting of the polycarbonate ribbon, ink layer, and Kapton substrate. This value of a is chosen to have the same order of magnitude as the thermal diffusivity of the carbon-loaded polycarbonate material, and it is then adjusted to give a good fit to experimental data. The thermal conductivity K' of the substrate is determined from  $K' = a \cdot C'$ , where C' is the heat capacity of the Kapton material. The different values of thermal conductivity between the ribbon and the Kapton substrate imply that the ink-Kapton interface acts effectively as a thermal barrier which regulates heat flow across it. Using the same area of  $2l \times 2w$  for both sources  $q'_1$  and  $q'_2$  and appropriately adjusting a to fit the peak ink temperature under an electrode, it was found that the calculated value of the ink temperature between the electrodes was always much lower than the measured value. These high temperatures measured between the electrodes can be accounted for by assuming a larger effective area A of the heat source at the bottom ribbon-ink interface as compared with an area of  $2l \times 2w$  for the top source at the electrode-ribbon contact. This effective area is thus the other adjustable parameter in the model, and physically it accounts for the increase in area due to the hot ink being squeezed out from under the electrodes due to head pressure.

Using values of parameters given in **Table 1**, we have calculated the ink temperature profiles for the center electrode in a group of three electrodes as a function of distance in the direction of motion for different printing

$$T_{1} = \frac{Q/C}{(4\pi at)^{1.5}} \exp -\left[\frac{(x-x_{0})^{2} + (y-y_{0})^{2} + (z-z_{0})^{2}}{4at}\right] + \frac{K-K'}{K+K'} \frac{Q/C}{(4\pi at)^{1.5}} \exp -\left[\frac{(x-x_{0})^{2} + (y-y_{0})^{2} + (z+z_{0})^{2}}{4at}\right] \qquad z \ge 0, \quad (1)$$

$$T_2 = \frac{2K}{K + K'} \frac{Q/C}{(4\pi at)^{1.5}} \exp\left[-\left[\frac{(x - x_0)^2 + (y - y_0)^2 + (z - z_0)^2}{4at}\right]\right] \qquad z < 0.$$
 (2)

 $T_{\rm r}(x, y, z, x_0, y_0)$ 

$$= T_{r1}(x, y, z, x_0, y_0) + T_{r2}(x, y, z, x_0, y_0),$$
 (3)

where

$$T_{rl}(x, y, z, x_0, y_0) = \frac{1}{(4\pi at)^{1.5}} \sum_{n=-\infty}^{\infty} Q_1/C \left\{ \left[ \frac{K - K'}{K + K'} \right]^{|n|} \exp \left[ - \left[ \frac{(x - x_0)^2 + (y - y_0)^2 + \{z - d_i - 2n(d_i + d_p)\}^2}{4at} \right] \right\} + \left[ \frac{K - K'}{K + K'} \right]^{|n-1|} \exp \left[ - \left[ \frac{(x - x_0)^2 + (y - y_0)^2 + \{z - d_i - 2n(d_i + d_p)\}^2}{4at} \right] \right\} , \tag{4}$$

and

$$T_{r2}(x, y, z, x_0, y_0) = \frac{1}{(4\pi at)^{1.5}} \sum_{n=-\infty}^{\infty} Q_2/C \left\{ \left[ \frac{K - K'}{K + K'} \right]^{|n|} \exp \left[ -\left[ \frac{(x - x_0)^2 + (y - y_0)^2 + \{z - (d_i + d_p) - 2n(d_i + d_p)\}^2}{4at} \right] + \left[ \frac{K - K'}{K + K'} \right]^{|n-1|} \exp \left[ -\left[ \frac{(x - x_0)^2 + (y - y_0)^2 + \{z + (d_i + d_p) - 2n(d_i + d_p)\}^2}{4at} \right] \right\}.$$
 (5)

 $T_{\rm m}(x, y, z, x_0, y_0)$ 

$$= T_{m1}(x, y, z, x_0, y_0) + T_{m2}(x, y, z, x_0, y_0),$$
 (6)

where

$$T_{m1}(x, y, z, x_0, y_0) = \frac{1}{4\pi a} \sum_{n=-\infty}^{\infty} q_1/C \left\{ \left[ \frac{K - K'}{K + K'} \right]^{|n|} (1/R_{1n}) \exp - \left[ \frac{R_{1n} - (x - x_0)}{2a/v} \right] + \left[ \frac{K - K'}{K + K'} \right]^{|n-1|} (1/R_{2n}) \exp - \left[ \frac{R_{2n} - (x - x_0)}{2a/v} \right] \right\},$$

$$T_{m2}(x, y, z, x_0, y_0) = \frac{1}{4\pi a} \sum_{n=-\infty}^{\infty} q_2/C \left\{ \left[ \frac{K - K'}{K + K'} \right]^{|n|} (1/R_{3n}) \exp - \left[ \frac{R_{3n} - (x - x_0)}{2a/v} \right] + \left[ \frac{K - K'}{K + K'} \right]^{|n-1|} (1/R_{4n}) \exp - \left[ \frac{R_{4n} - (x - x_0)}{2a/v} \right] \right\},$$

$$(8)$$

and

$$R_{1n}^{2} = (x - x_{0})^{2} + (y - y_{0})^{2} + [z - d_{i} - 2n(d_{i} + d_{p})]^{2},$$

$$R_{2n}^{2} = (x - x_{0})^{2} + (y - y_{0})^{2} + [z + d_{i} - 2n(d_{i} + d_{p})]^{2},$$

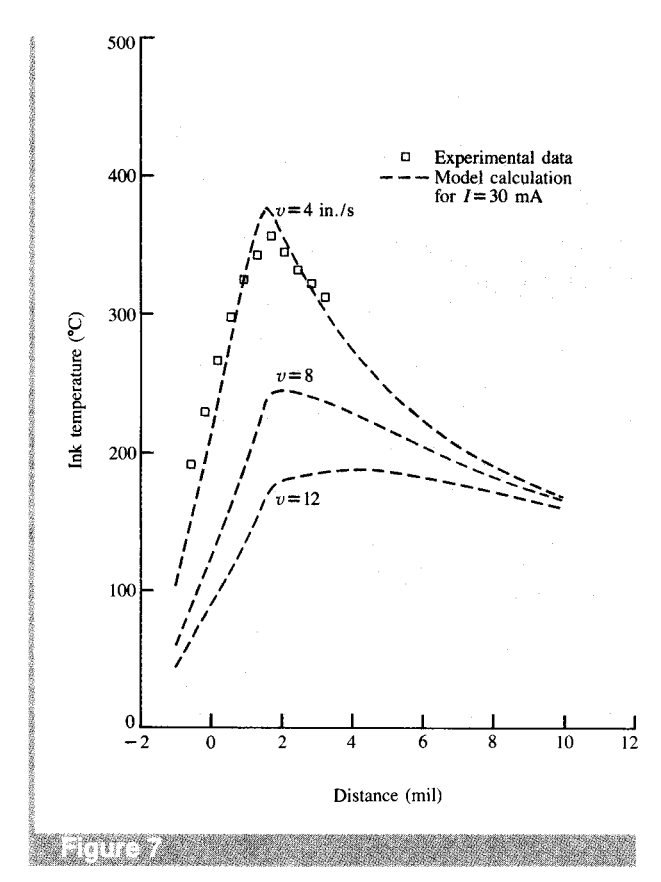
$$R_{3n}^{2} = (x - x_{0})^{2} + (y - y_{0})^{2} + [z - (d_{i} + d_{p}) - 2n(d_{i} + d_{p})]^{2},$$

$$R_{4n}^{2} = (x - x_{0})^{2} + (y - y_{0})^{2} + [z + (d_{i} + d_{p}) - 2n(d_{i} + d_{p})]^{2}.$$

$$(9)$$

$$T_{\mathbf{M}}(x, y, z, x_0, y_0) = \int_{-l}^{l} dx' \int_{-w}^{w} dy' T_{\mathbf{m}1}(x, y, z, x_0 - x', y_0 - y') + \int \int_{A} dx' dy' T_{\mathbf{m}2}(x, y, z, x_0 - x', y_0 - y'). \tag{10}$$

515



Calculated spatial profiles of ink temperature under an electrode in the direction of printing for various printing speeds. The spatial origin is at the electrode center. Data points represent measured values taken from Fig. 2.

**Table 1** Values of parameters used in the model.

Input current I	$30 \times 10^{-3} \text{ A}$
Current loss $I_{L}$	$2.0 \times 10^{-3} \text{ A}$
Ribbon thickness $d_{\rm p}$	15 μm
Ink thickness $d_i$	5 μm
Electrode spacing $Y_s$	100 μm
Electrode contact area $(2l \times 2w)$ for $q'_2$	$1.8 \times 2 \text{ mil}^2 \text{ or } 46 \times 50  \mu\text{m}^2$
Effective area $A$ for $q'_1$	$3.2 \times 3.5 \text{ mil}^2 \text{ or } 81 \times 89 \ \mu\text{m}^2$
Effective diffusivity a	$0.0025 \text{ cm}^2/\text{s}$
Conductivity K (Ribbon)	0.0046 (W/cm·s·K)
Conductivity K' (Kapton)	0.0037 (W/cm·s·K)
Heat input $q'_1$	$5.0 \times I^*/A \text{ (W/cm}^2)$
Heat input $q_2'$	$0.41 \times I \times v^{0.8}/2l \times 2w$

Effective current  $I^* = I - I_L$ Printing speed v (in./s) speeds. These profiles are illustrated in **Figure 7** for a current of 30 mA. The data points correspond to the measured values taken from Fig. 2 for a print current of 30.4 mA and a printing speed of 3.9 in./s. One observes that the value of the peak ink temperature decreases with increasing speeds, and that the position of the peak shifts away from the center of the active electrode. Also, the spatial decay profiles are flatter for higher printing speeds. To compensate for the decrease in peak ink temperature for high speed, one must increase the input current; e.g., a current as high as 69 mA is required to reach a peak temperature of 342°C at 16 in./s, as compared with a current of 28 mA at 4 in./s.

A comparison of the calculated results with experimental data corresponding to peak ink temperatures under the electrode is shown in Figure 8. The vertical axis corresponds to the ratio of effective input current  $I^*$  to the peak ink temperature rise, and the horizontal axis corresponds to printing speed. Here,  $I^*$  is defined as the input current I minus the current spreading loss  $I_L$ , and  $I_L$  was determined to be 2 mA from the intercept at ambient temperature of the peak ink temperature versus input current plots as shown in Fig. 4. There is a good agreement between the measured values and the calculated curve, and within a limited range the inverse of the temperature rise at constant current is approximately a linear function of speed.

The dependence of ink temperatures on ink thickness has also been incorporated in the model. The result of calculation shows that the peak ink temperature decreases from about 375°C to 288°C (at 4 in./s and 26 mA) as the ink thickness increases from 2.5 to 6.5  $\mu$ m, which agrees qualitatively with the experimental observation.

The dependence of ink temperatures on the number of active electrodes is accounted for in the model as the intrinsic thermal diffusion of heat conduction. However, the calculations including only thermal diffusion have underestimated this interaction. Thus, the model has to be expanded to include a more complete analysis of the lateral spreading phenomena, both electrical and thermal, to fully explain the experimental results.

## 4. Summary and conclusions

Dynamic measurements of ink temperatures in resistive ribbon thermal transfer printing have been carried out using an infrared radiometric microscope. A phenomenological model for the calculations of temperature profiles and equivalent currents over a wide range of printing speeds has been outlined for moving heat sources in a composite medium. The main results are as follow:

 Dynamic measurements of ink temperatures on Kapton allowed a direct estimation of ink temperatures during actual printing, at least on very smooth paper with reasonably good thermal contact with the ink.
 Underneath an electrode, the ink reaches a temperature

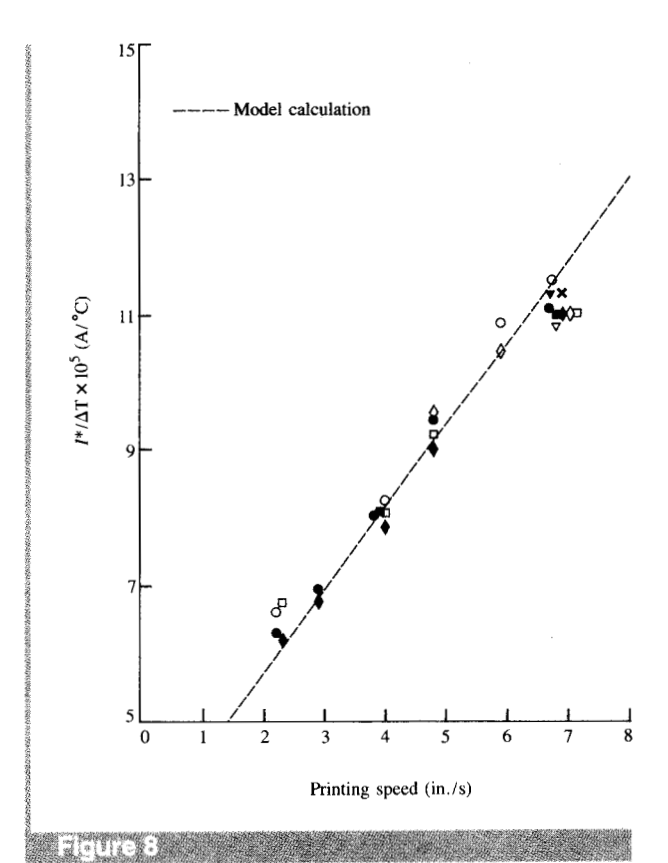
- as high as 380°C at an input current of 30 mA, but between the electrodes the ink temperatures are relatively low (~230°C).
- 2. The peak ink temperatures were observed to depend linearly on the total input current, suggesting a nonlinear element as the heat source. The polycarbonate-aluminum interface is essentially the primary heat source, with some secondary contribution from the nonlinear contact resistance at the top ribbon surface. Within the narrow range of 2 to 8 in./s, the peak ink temperatures were approximately proportional to the inverse of a linear function of speed.
- 3. A phenomenological model based on three-dimensional heat conduction theory for moving finite heat sources in a medium has been analyzed. This model assumed steady state temperatures in a uniform-diffusivity medium whose effective diffusivity was adjusted to simulate the multilayer structure consisting of the ribbon, ink layer, and Kapton substrate (each of which can have different heat capacities). When used to calculate the ink temperatures, it agreed well with the experiments. Further, the model permitted projections to be made of the current required to print over a wide range of printing speeds.

# **Acknowledgments**

The authors acknowledge the assistance of R. John in the initial experiments. They are also thankful to D. Dove, R. Laff, K. Shih, N. Caswell, R. Feigenblatt, and R. Lane for fruitful discussions.

## References and note

- J. L. Yoder and E. Webster, Thermal Transfer Printing: Technology, Products, Prospects, L. Mirowitz and F. A. Stefansson, Eds., DATEK Information Services, Inc., Newtonville, MA, 1983.
- L. Montanari and F. Knirsch, "Electro-Thermic Printing Device," U.S. Patent 3,744,611, 1973.
- 3. J. L. Mitchell and K. S. Pennington, "Thermal Transfer Printer Employing Special Ribbons with a Current Pulse," *IBM Tech. Disclosure Bull.* **18**, No. 8, 2695 (1976).
- K. S. Pennington and J. L. Mitchell, "Improved Printhead and Ribbon Structures for Thermal Transfer Printing Applications," *Research Report RC-5878*, IBM Thomas J. Watson Research Center, Yorktown Heights, NY, 1976.
- K. S. Pennington and W. Crooks, "Resistive Ribbon Thermal Transfer Printing (R2T2): A New Printing Technology," Technical Abstracts, Second International Congress on Non-Impact Printing, Society of Photographic Scientists and Engineers, Springfield, VA, 1984, p. 236.
- W. Crooks and K. S. Pennington, "Resistive Ribbon Thermal Transfer Printing, Ribbon and Head Requirements," *Technical Abstracts*, Second International Congress on Non-Impact Printing, Society of Photographic Scientists and Engineers, Springfield, VA, 1984, p. 237.
- \*Kapton is a registered trademark of E. I. du Pont de Nemours and Co., Inc., Wilmington, DE.
- C. D. Makowka, IBM System Products Division, Boca Raton, FL, private communication.
- R. Wooton, IBM Information Products Division, Lexington, KY, private communication.



Ratio of effective current to peak ink temperature rise versus printing speed. The points are experimental data on a Kapton substrate and the dashed line is from the model calculation.

- Robert A. Laff and Claus D. Makowka, "Thermal Behavior of Resistive Ribbon for Single-Stylus Excitation," *IBM J. Res. Develop.* 29, 527–537 (1985, this issue).
- B. M. Cassidy, IBM Information Products Division, Lexington, KY, private communication.
- K. K. Shih and D. B. Dove, IBM Research Division, Yorktown Heights, NY, private communication.
- H. S. Carslaw and J. C. Jaeger, Conduction of Heat in Solids, 2nd Ed., Clarendon Press, Oxford, England, 1959, Chs. X and XIII
- T. C. Chieu, IBM Thomas J. Watson Research Center, Yorktown Heights, NY, unpublished results.

Received October 1, 1984; revised March 27, 1985

**Trieu C. Chieu** *IBM Research Division, P.O. Box 218, Yorktown Heights, New York 10598.* Dr. Chieu joined IBM at the Thomas J. Watson Research Center, Yorktown Heights, New York, in 1983. He is presently a Research staff member in the printer materials

group of the I/O Technology Department. His research interests include the synthesis and investigation of solid state materials. He received his B.S., M.S., and Ph.D. degrees in electrical engineering from the Massachusetts Institute of Technology, Cambridge, in 1978, 1980, and 1983. Dr. Chieu is a member of the American Physical Society.

O. Sahni IBM Research Division, P.O. Box 218, Yorktown Heights, New York 10598. Dr. Sahni is a Research staff member in the Input/Output Technology Department at the Thomas J. Watson Research Center. He joined IBM Research in 1972 and was involved extensively, for almost a decade, in all aspects of the physics and technology of information output devices. His major contributions to this subject have been in the areas of gas discharge and thin-film electroluminescent displays. Prior to joining IBM, his research activity was in the fields of flame plasmas and gaseous electronics. He received an M.S. in physics in 1960 from the Banaras Hindu University, India, and an M.Eng. in electrical engineering in 1962 from the Indian Institute of Technology, Bombay. From 1963 to 1967, he was a Lecturer in the Department of Electrical Engineering at the Indian Institute of Technology, Bombay. From 1967 to 1969, he did research work in France at the Center for Nuclear Studies, Atomic Energy Commission, Saclay, and at the Laboratory for Plasma Physics, University of Paris, Orsay. He came to Rensselaer Polytechnic Institute, Troy, New York, in 1969, receiving a Ph.D. in electrophysics in 1972. Dr. Sahni was a recipient of the 1983 Special Recognition Award from the Society for Information Display, and an IBM Outstanding Technical Achievement Award for his work on gas discharge display devices. He is a senior member of the Institute of Electrical and Electronics Engineers, and a member of the American Physical Society, Sigma Xi, and the Society for Information Display.